Materials Science in Semiconductor Processing 144 (2022) 106628

Contents lists available at ScienceDirect

Materials Science in Semiconductor Processing

journal homepage: www.elsevier.com/locate/mssp

A general strategy for polishing SiC wafers to atomic smoothness with arbitrary facets

Peixuan Ji, Kaimin Zhang, Zhenzhen Zhang, Mei Zhao, Rui Li, Danni Hao, Ramiro Moro, Yanqing Ma, Lei Ma *

Tianjin International Center for Nanoparticles and Nanosystems, Tianjin University, 92 Weijin Road, Nankai District, Tianjin, 300072, China

ARTICLE INFO

Keywords:
Silicon carbide
Arbitrary facets
Chemical mechanical polishing
Material removal rate

ABSTRACT

SiC is essential for epitaxial growth of graphene and promises to be an ideal material for next generation high-power electronics. The electronic properties of graphene are highly dependent on the facet on which it is grown. Therefore, the selection of facet provides an extra tuning parameter to obtain its desired characteristics. As one of the key factors of growing pristine graphene on SiC wafers, their roughness requires to be atomically smooth. In this work, we present a data-driven study of the grinding, mechanical polishing and chemical mechanical polishing (CMP) procedures applied to a SiC wafer with arbitrary facets. The phenomena and principles in the polishing steps are discussed. As specific facets of SiC have unique atomic arrangements, different recipes are required for the C and Si faces and their performances are investigated. The interesting, but rarely studied ($1\bar{1}05$) facet is taken as an example of a non-polar case to apply the procedures. It is found that the material removal rate (MRR) in mechanical polishing is directly related to the facet hardness. Hence, the MRR of the ($1\bar{1}05$) facet is the slowest in that process, however, during CMP its MRR is 18 times faster than the Si-face, hints the different chemical and physical polishing mechanism. Accordingly, polishing recipes are proposed that can be adjusted to create atomically smooth wafers of arbitrary facets of SiC.

1. Introduction

Silicon as the present dominant platform plays the most critical role in the microelectromechanical industry due to its favorable electrical and mechanical properties [1]. However, in high power devices, structure disorder and dopants diffusion at high temperatures can severely deteriorate its electronic performance and even lead to permanent damage. In contrast, silicon carbide (SiC) owns much better mechanical properties and thermodynamic stability. It is capable of being used as an electrical semiconductor to well outperform silicon at much higher working temperature, even keeping extremely low diffusivity up to 600 °C [2]. Also, SiC is highly resistive to a broad spectrum of chemicals with outstanding high-temperature oxidative endurance. These advantages make SiC a practical substitute of Si for electronics applications in environments of high temperatures, corrosive, and intensive radiation [3,4]. Moreover, SiC is the primary material to epitaxially grow graphene for epi-graphene-based devices. Its use in microelectronics requires the surface roughness being less than a nanometer and defect free to avoid interference to the epi-layer [5]. Hence, surface preparation of the wafer is a critical step in electronic integration fabrication [6]. However, also due to its extraordinary mechanical robustness and chemical resistance, shaping and polishing SiC is very challenging [7]. Additionally, different facets of SiC have different material removal rates, which further raise the difficulties for fine mechanical processing.

After dicing, damages on the SiC wafer surface could take many forms, such as scratches, pits, film interfaces delamination, and chemical or particulate impurities implantation [8]. Post processing, such as hydrogen etching, high temperature annealing and chemical mechanical polishing (CMP) are commonly adopted approaches to planarize the SiC wafer. The CMP method combines chemical reactions with mechanical removal [9], in which an oxide film forms on the sample surface and is followed by polishing with a soft abrasive [10,11]. Compared to hydrogen etching, CMP has the advantage of better preserving the intrinsic properties of the grown graphene [12]. Also, there is no need for high temperatures, which is inevitable for both hydrogen etching and annealing and known for the critical requirement of step formation in the planarization procedure [13–15]. CMP can effectively eliminate shallow scratches caused by mechanical polishing without introducing

* Corresponding author.
E-mail address: lei.ma@tju.edu.cn (L. Ma).

https://doi.org/10.1016/j.mssp.2022.106628
Received 6 April 2021; Received in revised form 9 June 2021; Accepted 6 March 2022
Available online 9 March 2022

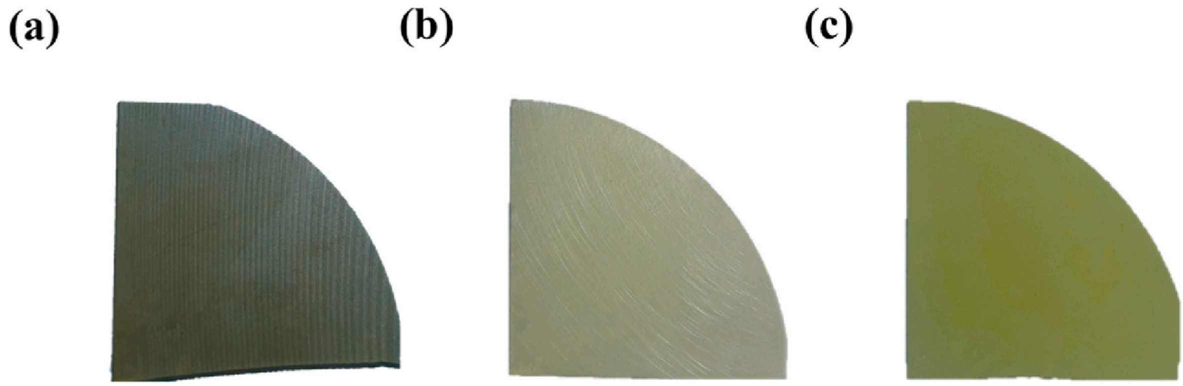

Fig. 1. (a) 4H–SiC crystal after dicing; (b) SiC wafer after grinding; (c) SiC wafer after CMP.

extra subsurface damage [12] and largely reduce the amount of defects [16]. Therefore, CMP is considered as the ideal way of SiC wafer planarization.

In the past several decades, much progress has been achieved for polishing on both the silicon face and carbon face of SiC. It is easier to get ultra-flat surfaces on the Si-face than C-face by CMP, and the Si-face is also considered to have broader application spectrum for device fabrication or as substrate for epitaxial film growth. Shi et al. [17] and Zhou et al. [18] demonstrated that the polished Si-face consists of regular step terraces with surface roughness of about 50 p.m. Deng et al. employed electro-chemical mechanical polishing by combining anodic oxidation and a soft abrasive to polish the Si face, obtaining a root mean square roughness of 0.23 nm [19]. Later, the same group reported an alternative recipe combining thermal oxidation pre-treatment and a soft abrasive polishing for the C-face, obtaining a surface roughness of 0.75 nm with the surface pits density of 1 per 5 μm diameter area [20]. Theoretically, Preston presented the first empirical mechanical model, which built the connection between the removal rate and the frictional force on the polishing pad [21]. Luo et al. conceived a model that demonstrated the dependence of removal rate on the abrasive size and the elastic deformation of the pad [22]. Both experimental and theoretical works indicate that abrasive mechanical properties, particle size, the topography of the polishing pad, pad speed and contact pressure are the predominant factors for the removal rate of the polished surface [23,24]. These factors also determine the surface quality, including flatness, uniformity, roughness, and subsurface damage of SiC [18].

The successful planarization of an arbitrary facet of SiC has been a long-standing challenge. Here, we present a successful recipe for atomically flat polishing arbitrary facets of SiC. A simplified approach with three steps is proposed to planarize the surface, which include abrasive pad grinding, abrasive slurry polishing and CMP, achieving 0.05 nm roughness on the Si-face and 0.12 nm on the C-face. In particular, a series of recipes have been systematically tested on an interesting but rarely studied non-polar face (N-face) with lattice constant ($1\ \bar{1}\ 05$). This extends the toolbox for future exploiting silicon carbide both for next generation of wide band gap semiconductors and epi-graphene based electronics.

2. Experiments

Single-crystal rods of SiC (n-doped 4H–SiC) were used as raw material. The process starts by dicing the SiC rod into wafers with the desired facet by a diamond wire saw [26]. The planarization process is divided into three steps: grinding, mechanical polishing and chemical mechanical polishing. Fig. 1 shows the surfaces after each step. All recipes are conducted using the polishing machine Buehler's EcoMet 250Pro.

In order to remove visible scratches, as seen in Fig. 1(a), which are introduced by the dicing process, the first step is pure mechanical

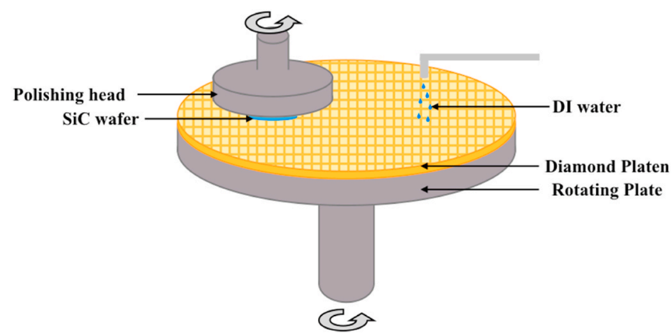

Fig. 2. Schematic diagram of grinding.

grinding. The initial size of material for polishing is 500 μm thick and one quarter of a 2-inch diameter round wafer, with the requested orientation or facet. The wafer was waxed onto the platen of the polishing machine using paraffin. It is shown schematically in Fig. 2.

All facets share the same optimized mechanical-parameter settings for grinding, including down-pressuring force (DPF), rotating speed of the polishing head (PH), bottom supporting plate (BSP) and slurry supplying rate (SSR). In the grinding process, the wafers were polished by a diamond platen with a supply of distilled water. DPF was 50 N, the rotating speed of the PH was 60 rpm, and 280 rpm for BSP, the supply rate of DI water is 550 ml/min. This is followed by mechanical polishing, where the polishing pad is made of silk (microscopic image shown in Fig. 3(a)) with 3 μm, 1 μm and 0.05 μm diamond slurries. The DPF was 30 N, PH speed was 60 rpm, BSP speed was 260 rpm and SSR was 1.5 ml/min.

As for CMP process, the polishing pad is made of fur (microscopic image shown in Fig. 3(b)) with colloidal silica suspension slurry. The slurry is a mixture of H_2O_2, colloidal silica (SiO_2) particles with 100 nm diameter average size, and KOH (Fig. 4). The pH of colloidal silica slurry is 10.0. The PH speed was 60 rpm, the BSP speed was 90 rpm and SSR was 15 ml/min. The reactions taking place during CMP are presented as follows [25,27,28].

$$4H_2O_2 + 4e^- \rightarrow 4OH^- + 2H_2$$

$$Si + 2OH^- \rightarrow Si(OH)_2^{2+} + 2e^-$$

$$Si(OH)_2^{2+} + 2OH^- \rightarrow Si(OH)_4 + 2e^-$$

H_2O_2 as the strong oxidant to provide OH^-, but there have been studies that show the MRR increases with adding KOH into the slurry. Silica colloidal slurry without alkali addition shows lack of ability to remove SiC [29]. SiO_2 particles provide mechanical remove effect for CMP process. Therefore, the ingredients of slurry (SiO_2 particles, H_2O_2 and KOH) all have influence on SiC planarization behavior.

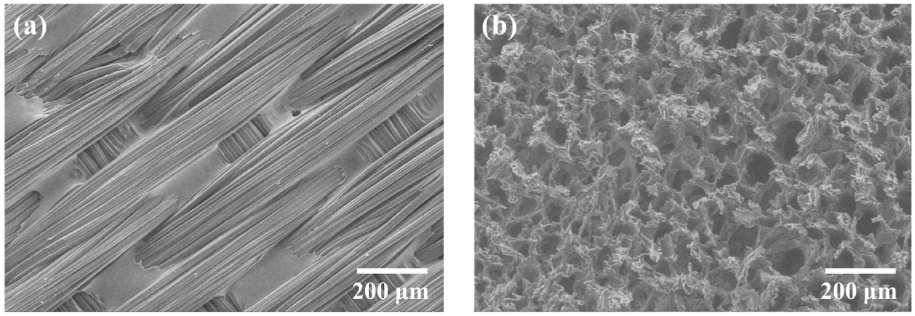

Fig. 3. SEM images of silk polishing pad (a) and fur polishing pad (b).

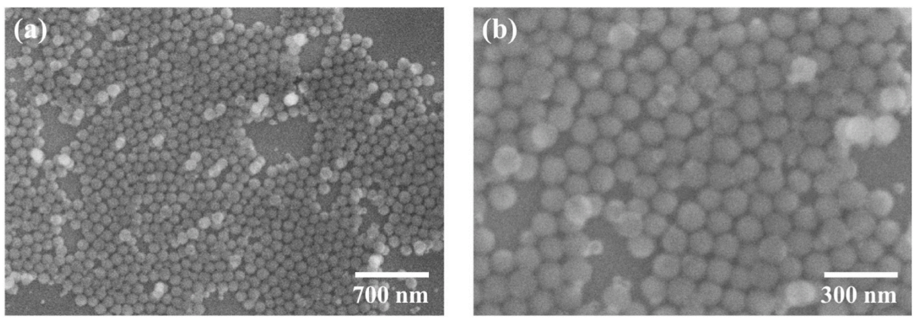

Fig. 4. SEM images of SiO_2 particles (a) (b).

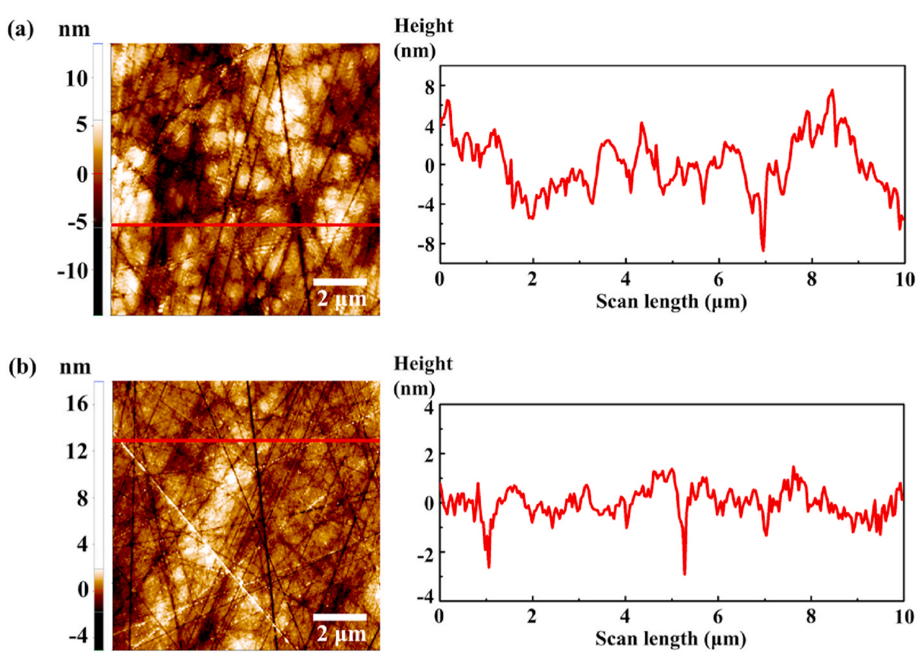

Fig. 5. AFM images and profiles of the Si face after polishing with a 3 μm diamond suspension (Ra:2.7 nm) (a), and 1 μm diamond suspension (Ra: 0.67 nm) (b).

After the polishing procedure, the wafers were ultrasonically cleaned with acetone, isopropanol and deionized water, then dried up. To evaluate the surface quality, an atomic force microscope (AFM) is used to inspect the surface. The polishing time to get a certain uniformity/roughness is used to calculate the material removal rate (MRR).

3. Results and discussion

3.1. Comparison of MRR in grinding and mechanical polishing processes between Si face, C face and (1 $\overline{1}$ 0n) facet

In the grinding process, a diamond platen was used to remove deep scratches caused by wire cutting. In order to avoid causing internal cracks in the crystal, the applied DPF was less than 80 N. The indication of procedure completion to continue the mechanical polishing is no visible scratches on the wafer. We calculate the time to remove scratches

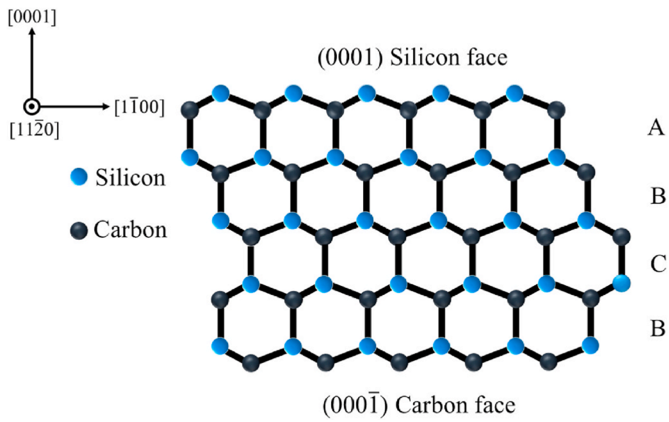

Fig. 6. Atomic structure of 4H–SiC. Silicon atoms are shown in blue, whereas Carbon atoms are in black.

which caused by dicing from SiC rods. Due to different facets have different hardness, C-face needed the least time to achieve surface flatness at this stage, while the non-polar face needed the longest. The surfaces were still very rough after grinding, so there was no obvious topographic distinction between the different faces from Scanning Electron Microscope (SEM, Hitachi 3500) images.

To remove nanometer-scale scratches, different sized diamond suspensions were employed in mechanical polishing. For the Si face, 9 μm, 3 μm, 1 μm and 0.05 μm diamond suspensions were tested sequentially. Due to the shallow pits of the silk pad, as shown in Fig. 3(a), it is hard to hold polishing particles in position, especially for large particles. Therefore, silk pads with 9 μm diamond slurry have much less MRR than with 3 μm [23]. Further polishing the Si-face with 0.05 μm diamond suspension does not improve the surface roughness after polishing with 1 μm. This simplified the original multiple step mechanical polishing to adjust it to two steps for the Si-face instead. Fig. 5 shows the topography of the Si-face after 3 μm and 1 μm diamond suspension polishing.

The C-face is terminated by a layer of carbon (Fig. 6) and the (1 $\bar{1}$ 05) facet appears similar to the Si-face but rotated 37.1°. The same mechanical polishing process was applied to both the C-face and the (1$\bar{1}$ 05) facet using 3 μm, 1 μm and 0.05 μm diamond slurries sequentially. After polishing with 3 μm diamond slurry, the surface of the C-face already has fewer shallow scratches per unit area compared with the Si-face while the deepest ones can reach about 10 nm, almost the same as the results of Si-face. However, in the case of the C-face, the 0.05 μm diamond slurry does improve the smoothness effectively (see Fig. 7 (a), (b) and (c)). The (1 $\bar{1}$ 05) facet takes the most time grinding due to its higher hardness and there is almost no effect by polishing with 0.05 μm diamond slurry. Its roughness reaches 0.51 nm after polishing with 1 μm diamond slurry (Fig. 7 (e)), which is comparable to the result of Si face (Fig. 5(b)). At this stage, the optimum is to achieve an MRR higher than the generation rate of new scratches and the results indicate that the MRR of grinding and mechanical polishing is with the order of C-face > Si-face > (1 $\bar{1}$ 05) facet.

3.2. Comparison between the MRR of CMP of the Si face and the (1 $\bar{1}$ 0n) facet

After mechanical polishing, the surface roughness is about 0.5 to 1 nm for both the Si-face and the (1 $\bar{1}$ 05) facet, while it was about 0.2 to 0.5 nm for the C-face. However, they are still not smooth enough to be appropriate substrates for epitaxial growth of graphene. CMP was adopted to further flatten the surface with minimum introduction of new damages. For this procedure, Y. Zhao et al. have shown that the MRR is more sensitive to the slurry particle size than the applied force and the speeds of PH and BSP [30] and F.G. Shi et al. found that the polishing rate dependence on force is nonlinear and highly correlated to the number of particles in contact with the wafer [31], which will need to be considered.

Small size abrasives are inefficient in mechanical removal, while larger ones are more efficient, but at the cost of diminishing planarization quality. It usually reflects as larger mean crack lengths from subsurface damage with increase in abrasive size [32,33]. The material removal rate depends on the chemical etching rate (CER) of SiC with the CMP slurry. In this experiment, 100 nm colloidal silica abrasive slurry was chosen, as shown in Fig. 4. The C-face is hard to be flattened by CMP mainly due to inertness of the carbon-terminated layer to OH^- [34], which hinders the surface reactions, hence slowing down the MRR.

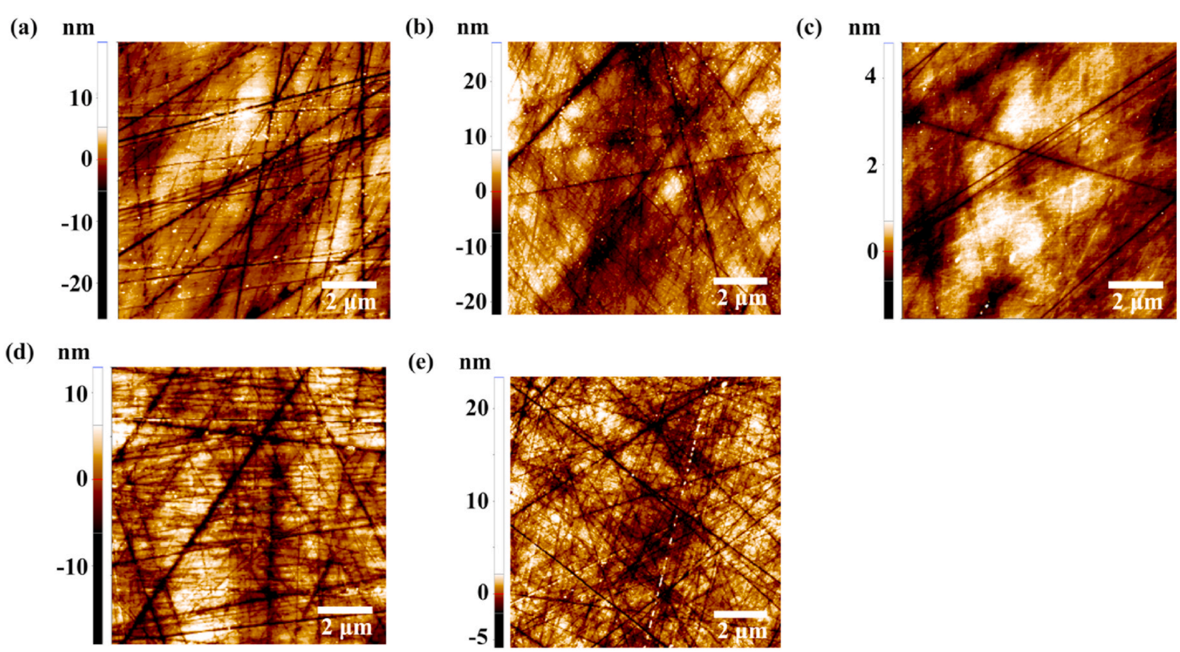

Fig. 7. AFM images of the C-face after polishing with 3 μm diamond slurry (a), 1 μm diamond slurry (b), 0.05 μm diamond slurry (R_a:0.281 nm) (c), and non-polar face after polishing with 3 μm diamond slurry (d) and 1 μm diamond slurry (e).

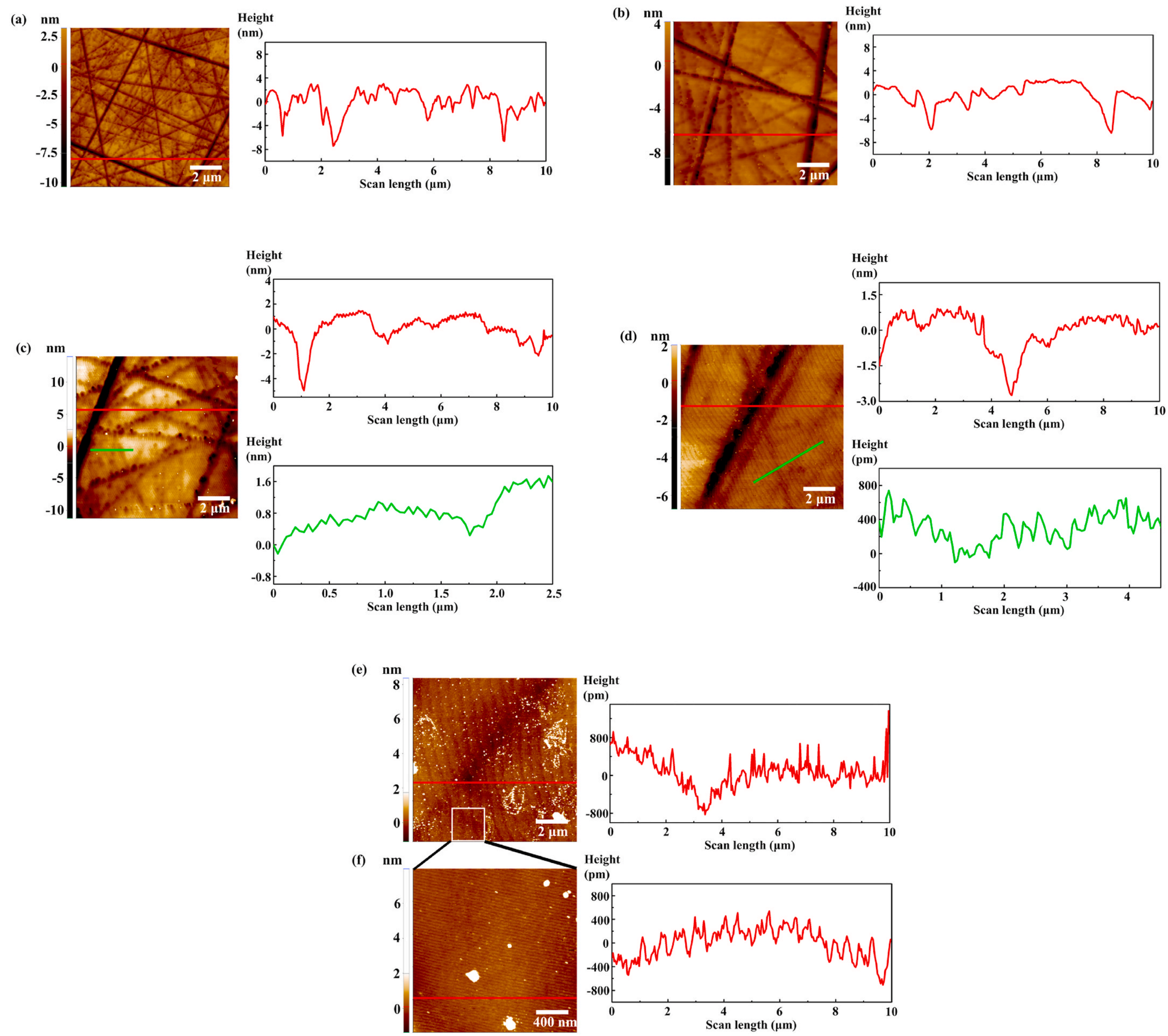

Fig. 8. AFM images of the Si face after using colloidal silica suspension for 1 h (a), 3 h (b), 5 h (c), 7 h (d) and 9 h (e, f).

For the Si-face it is noticeable that the total number of scratches on the surface decreased after 3 h of CMP compared to 1h, but the number of deepest scratches increased (Fig. 8(a)(b)). There is a proposed hypothesis for this phenomenon. First, the deepest scratches come from initially non-visible (in AFM images) sub-surface damage [35]. For shallow scratches, they are first transformed to discontinuous scratches which are further transformed into micro pits and are finally removed. However, deep scratches are first broadened and then transformed to wide and deep grooves. These grooves will further transform into discontinuous scratches, then micro pits and finally are removed [36].

Regular terraces start to show on the Si-face after 5 h of CMP (Fig. 8(c)). With longer polishing time, the depth of the deepest scratches become shallower (Fig. 8(d)(e)) until they are not detectable (Fig. 8(f)). The terrace orientation and step height are shown in Fig. 8(d–f). Fig. 8(d) shows the same terrace as in Fig. 8(e), but in a small area, while Fig. 8(e) shows a different orientation, and the height of the steps is 0.25 nm, corresponding to the thickness of Si–C bilayer [18]. The width between steps is 0.12 nm which corresponds to the size of silicon atoms which indicates a one-atom thick step, as shown in Fig. 8(f). The terraces may arise from the wafer miss-cut as shown in Fig. 8(d and e). The MRR was about 1–2 nm/h [6].

In order to make a comparative investigation on the influence of crystal facet orientation to the MRR of CMP, all the parameters were set the same for both Si face and $(1\,\bar{1}\,0n)$ facet. Comparing to the Si-face, the $(1\,\bar{1}\,05)$ facet is much easier to be polished. It only took 30 min to reach atomic level smoothness with the same CMP recipe, which is 18 times faster than the Si-face.

In the CMP process for SiC, the MRR is mainly determined by the reaction rate between OH^- and Si, which forms a softer layer and is eventually removed by abrasives. Since, $(1\,\bar{1}\,05)$ facet has more dangling bonds than the Si-face, leads to more active chemical reaction [34], which explains the much faster MRR for the N-face comparing to the Si-face.

For the N-face, the CMP reduces scratches to 1 nm from the previous step of mechanical polishing within 5 min, indicating an ultra-fast MRR. And then, these 1 nm scratches could be removed in the next 25 min. However, in the second step (10 min), some new scratches are

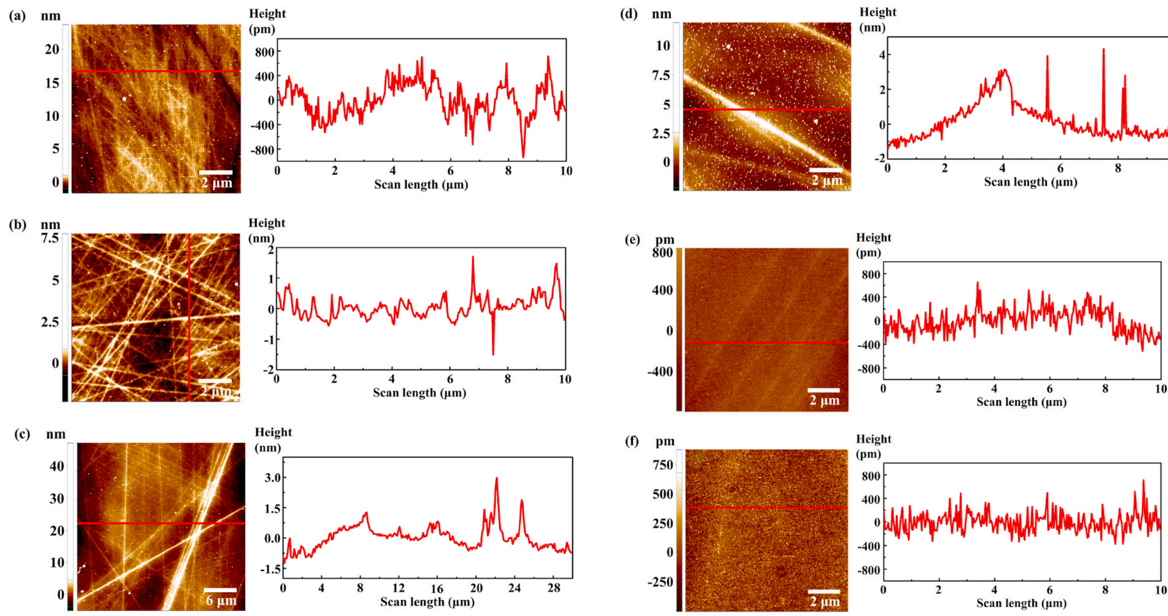

Fig. 9. AFM images of N-face after CMP with colloidal silica suspension for 5 min (a), 10 min (b), 15 min (c), 20 min (d), 25 min (e) and 30 min (f).

Table 1
Summary of the procedure parameters for polishing the three facets investigated.

Facet/ Procedure	Si-face	C-face	N-face	Comments
Grinding Force 50 N PH: 60 rpm, BSP: 280 rpm	Intermediate time	Least time	Longest time	MRR is correlated with hardness
Results	No visible scratches	No visible scratches	No visible scratches	
Mechanical Polishing Force 30 N PH: 60 rpm, BSP: 260 rpm	3 μm and 1 μm slurries	3 μm, 1 μm and 0.05 μm slurries	3 μm and 1 μm slurries	
Results	0.5–1 nm smoothness	0.2–0.5 nm smoothness	0.5–1 nm smoothness	
Chemical Mechanical Polishing 100 nm abrasive Force 30 N PH: 60 rpm, BSP: 90 rpm	9 h		30 min	CMP took much less time for the N-facet
Results	Atomic Smoothness		Atomic Smoothness	

introduced that showed as the bulgy lines in the AFM profiles (Fig. 9). These may be caused by an over-reaction of the slurry with the polishing face, leading to penetration of several layers due to the existence of large amount of surface dangling bonds. Most of the scratches were removed in the third step (15 min), but there are still some humps. They finally were completely removed in the last 15 min of CMP. It is worth noting that it took less time if there were no interruptions in the process, which were needed to observe the changes every 5 min, but Si and OH^- may not completely react in that time. In summary, the surface could reach atomic smoothness in 30 min of CMP. The optimized parameters are summarized in Table1.

4. Conclusion

The facet orientation of SiC determines the material removal rate (MRR) and the final surface quality after polishing. In this work, the MRR mechanism was explored with the Si and C faces, and accordingly the determined recipe was applied to polish the facet (1 $\bar{1}$ 05), which achieved atomic smoothness successfully.

It was found that the different facets display distinct MRR of grinding, mechanical polishing and CMP. For grinding and mechanical polishing, due to the dominant role of friction, the facet-dependent hardness defines the MRR, confirming that the order of MRR during these procedures is C face > Si face> (1 $\bar{1}$ 0n) facet. Regarding CMP, the MRR and final surface quality are mainly governed by the chemical reaction rate of silicon to the slurry, the fiber texture and material of polishing pad, the slurry abrasive size and supply rate and the polishing time. Due to the fact that the (1 $\bar{1}$ 05) facet has many more dangling bonds compared with the Si-face, which results in much higher chemical activity, it leads to a much faster MRR for the N-face. These results open an avenue to many varieties of non-polar graphene growth and applications of SiC with different facets, which will vastly extend the possibilities of epi-graphene and SiC based devices for next generation high speed and power electronics.

Credit: author statement

Peixuan Ji: Methodology, Investigation, Data curation, Writing–original draft preparation.
Kaimin Zhang: Investigation, Data curation.
Zhenzhen Zhang: Investigation, Data curation.
Mei Zhao: Investigation, Data curation.
Rui Li: Investigation, Data curation.
Danni Hao: Writing-review & editing.
Ramiro Moro: Writing-review & editing.
Yanqing Ma: Validation, Writing-review & editing.
Lei Ma: Conceptualization, Supervision, Methodology, Validation, Writing-review & editing, Funding acquisition, project administration.

Declaration of competing interest

The authors declare that they have no known competing financial interests or personal relationships that could have appeared to influence the work reported in this paper.

Acknowledgment

This work was supported by the National Natural Science Foundation of China (No. 11774255) and Key Project of Natural Science Foundation of Tianjin City (No.17JCZDJC30100).

References

[1] M. Mehregany, X.A. Fu, L. Chen, Silicon carbide micro/nano systems for harsh environment and demanding applications, 2006 NSTI Nanotechnol, in: Conf. Trade Show - NSTI Nanotech 2006 Tech. Proc. vol. 3, 2006, pp. 471–474.

[2] R. Yamada, N. Igawa, T. Taguchi, S. Jitsukawa, Highly thermal conductive, sintered SiC fiber-reinforced 3D-SiC/SiC composites: experiments and finite-element analysis of the thermal diffusivity/conductivity, J. Nucl. Mater. 307–311 (2002) 1215–1220, https://doi.org/10.1016/S0022-3115(02)00957-1.

[3] Y. Katoh, L.L. Snead, I. Szlufarska, W.J. Weber, Radiation effects in SiC for nuclear structural applications, Curr. Opin. Solid State Mater. Sci. 16 (2012) 143–152, https://doi.org/10.1016/j.cossms.2012.03.005.

[4] T. Dinh, T.K. Nguyen, H.P. Phan, Q. Nguyen, J. Han, S. Dimitrijev, N.T. Nguyen, D. V. Dao, Thermoresistance of p-type 4H–SiC integrated MEMS devices for high-temperature sensing, Adv. Energy Mater. 21 (2019) 1–7, https://doi.org/10.1002/adem.201801049.

[5] M.B.J. Wijesundara, R. Azevedo, Silicon Carbide Microsystems for Harsh Environments, Springer, New York, 2011, https://doi.org/10.1007/978-1-4419-7121-0.

[6] X. Shi, G. Pan, Y. Zhou, C. Zou, H. Gong, Extended study of the atomic step-terrace structure on hexagonal SiC (0001) by chemical-mechanical planarization, Appl. Surf. Sci. 284 (2013) 195–206, https://doi.org/10.1016/j.apsusc.2013.07.080.

[7] L. Zhou, V. Audurier, P. Pirouz, J.A. Powell, Chemomechanical polishing of silicon carbide, J. Electrochem. Soc. 144 (1997), https://doi.org/10.1149/1.1837711.

[8] J.M. Steigerwald, S.P. Murarka, R.J. Gutmann, Chemical Mechanical Planarization of Microelectronic Materials, John Wiely & Sons, New York, 1997, https://doi.org/10.1002/9783527617746.

[9] H.H. Gatzen, K.H. Wu, S. Cvetkovic, Modeling CMP - investigation of the mechanical removal mechanism, in: Proc. 20th Annu. ASPE Meet. ASPE 2005, 2005, pp. 6–9.

[10] H.J. Kim, Abrasive for chemical mechanical polishing, in: A. Rudawska (Ed.), AbrasiveTechnology: Characteristics and Applications, IntechOpen, 2018, p. 183, https://doi.org/10.5772/intechopen.75408.

[11] K. Qin, B. Moudgil, C.W. Park, A chemical mechanical polishing model incorporating both the chemical and mechanical effects, Thin Solid Films 446 (2004) 277–286, https://doi.org/10.1016/j.tsf.2003.09.060.

[12] M. Kruskopf, K. Pierz, S. Wundrack, R. Stosch, J. Baringhaus, C. Tegenkamp, F. J. Ahlers, H.W. Schumacher, Epitaxial graphene on SiC : modification of Epitaxial graphene on SiC : modification of structural and electron transport properties by substrate pretreatment, J. Phys. Condens. Matter 27 (2015) 185303, https://doi.org/10.1088/0953-8984/27/18/185303.

[13] K.V. Emtsev, A. Bostwick, K. Horn, J. Jobst, G.L. Kellogg, L. Ley, J.L. McChesney, T. Ohta, S.A. Reshanov, J. Röhrl, E. Rotenberg, A.K. Schmid, D. Waldmann, H. B. Weber, T. Seyller, Towards wafer-size graphene layers by atmospheric pressure graphitization of silicon carbide, Nat. Mater. 8 (2009) 203–207, https://doi.org/10.1038/nmat2382.

[14] C. Çelebi, C. Yanik, A.G. Demirkol, I.I. Kaya, The effect of a SiC cap on the growth of epitaxial graphene on SiC in ultra high vacuum, Carbon 50 (2012) 3026–3031, https://doi.org/10.1016/j.carbon.2012.02.088.

[15] X.Z. Yu, C.G. Hwang, C.M. Jozwiak, A. Köhl, A.K. Schmid, A. Lanzara, New synthesis method for the growth of epitaxial graphene, J. Electron. Spectrosc. Relat. Phenom. 184 (2011) 100–106, https://doi.org/10.1016/j.elspec.2010.12.034.

[16] D.S. Dhami, B.S. Pabla, Material removal by chemical mechanical polishing-A review, Int. J. Adv. Res. Technol. 1 (2012) 1–8.

[17] X. Shi, G. Pan, Y. Zhou, Z. Gu, H. Gong, C. Zou, Characterization of colloidal silica abrasives with different sizes and their chemical-mechanical polishing performance on 4H-SiC (0001), Appl. Surf. Sci. 307 (2014) 414–427, https://doi.org/10.1016/j.apsusc.2014.04.048.

[18] Y. Zhou, G. Pan, X. Shi, S. Zhang, H. Gong, G. Luo, Effects of ultra-smooth surface atomic step morphology on chemical mechanical polishing (CMP) performances of sapphire and SiC wafers, Tribol. Int. 87 (2015) 145–150, https://doi.org/10.1016/j.triboint.2015.02.013.

[19] H. Deng, K. Hosoya, Y. Imanishi, K. Endo, K. Yamamura, Electro-chemical mechanical polishing of single-crystal SiC using CeO_2 slurry, Electrochem. Commun. 52 (2015) 5–8, https://doi.org/10.1016/j.elecom.2015.01.002.

[20] H. Deng, N. Liu, K. Endo, K. Yamamura, Atomic-scale finishing of carbon face of single crystal SiC by combination of thermal oxidation pretreatment and slurry polishing, Appl. Surf. Sci. 434 (2018) 40–48, https://doi.org/10.1016/j.apsusc.2017.10.159.

[21] F. Preston, The theory and design of plate glass polishing machine, J. Soc. Glas. Tech. 11 (1927).

[22] J. Luo, D.A. Dornfeld, Material removal mechanism in chemical mechanical polishing: theory and modeling, IEEE Trans. Semicond. Manuf. 14 (2001) 112–133, https://doi.org/10.1109/66.920723.

[23] Y. Xie, B. Bhushan, Effects of particle size, polishing pad and contact pressure in free abrasive polishing, Wear 200 (1996) 281–295.

[24] C. Wang, P. Sherman, A. Chandra, D. Dornfeld, Pad surface roughness and slurry particle size distribution effects on material removal rate in chemical mechanical planarization, CIRP Ann 54 (2005) 309–312, https://doi.org/10.1016/S0007-8506(07)60110-3.

[25] D. Zhao, X. Lu, Chemical mechanical polishing: theory and experiment, Friction 1 (2013) 306–326, https://doi.org/10.1007/s40544-013-0035-x.

[26] H. Huang, Y. Zhang, X. Xu, Experimental investigation on the machining characteristics of single-crystal SiC sawing with the fixed diamond wire, 2015, pp. 955–965. https://doi.org/10.1007/s00170-015-7250-8.

[27] H. Seidel, L. Csepregi, A. Heuberger, H. Baumgärtel, Anisotropic etching of crystalline silicon in alkaline solutions: I . Orientation dependence and behavior of passivation layers, J. Electrochem. Soc. 137 (1990) 3612–3626, https://doi.org/10.1149/1.2086277.

[28] Y. Wanga, L.C. Zhangb, A. Biddutc, Chemical effect on the material removal rate in the CMP of silicon wafers, Wear 270 (2011) 312–316, https://doi.org/10.1016/j.wear.2010.11.006.

[29] G. Pan, Y. Zhou, G. Luo, X. Shi, C. Zou, H. Gong, Chemical mechanical polishing (CMP) of on-axis Si-face 6H-SiC wafer for obtaining atomically flat defect-free surface, J. Mater. Sci. Mater. Electron. 24 (2013) 5040–5047, https://doi.org/10.1007/s10854-013-1519-1.

[30] Y. Zhao, L. Chang, A micro-contact and wear model for chemical-mechanical polishing of silicon wafers, Wear 252 (2002) 220–226, https://doi.org/10.1016/S0043-1648(01)00871-7.

[31] F.G. Shi, B. Zhao, Modeling of chemical-mechanical polishing with soft pads, Appl. Phys. A 67 (1998) 249–252, https://doi.org/10.1007/s003390050766.

[32] T. Suratwala, L. Wong, P. Miller, M.D. Feit, J. Menapace, R. Steele, P. Davis, D. Walmer, Sub-surface mechanical damage distributions during grinding of fused silica, J. Non-Cryst. Solids 352 (2006) 5601–5617, https://doi.org/10.1016/j.jnoncrysol.2006.09.012.

[33] R.K. Singh, S.-M. Lee, K.-S. Choi, G. Bahar Basim, W. Choi, Z. Chen, B.M. Moudgil, Fundamentals of slurry design for CMP of metal and dielectric materials, MRS Bull. 27 (2002) 752–760, https://doi.org/10.1557/mrs2002.245.

[34] X.F. Chen, X.G. Xu, X.B. Hu, J. Li, S.Z. Jiang, L.N. Ning, Y.M. Wang, M.H. Jiang, Anisotropy of chemical mechanical polishing in silicon carbide substrates, Mater. Sci. Eng. B 142 (2007) 28–30, https://doi.org/10.1016/j.mseb.2007.06.015.

[35] D. Ricci, P.C. Braga, Atomic force microscopy biomedical methods and applications, Methods Mol. Biol. 242 (2004) 298–302, https://doi.org/10.1385/1-59259-077-2, 199.

[36] H. Deng, N. Liu, K. Endo, K. Yamamura, Atomic-scale finishing of carbon face of single crystal SiC by combination of thermal oxidation pretreatment and slurry polishing, Appl. Surf. Sci. 434 (2018) 40–48, https://doi.org/10.1016/j.apsusc.2017.10.159.